

Active wave-guiding of piezoelectric phononic crystals

Joo Hwan Oh, Il Kyu Lee, Pyung Sik Ma, and Yoon Young Kim

Citation: [Applied Physics Letters](#) **99**, 083505 (2011); doi: 10.1063/1.3630231

View online: <http://dx.doi.org/10.1063/1.3630231>

View Table of Contents: <http://scitation.aip.org/content/aip/journal/apl/99/8?ver=pdfcov>

Published by the [AIP Publishing](#)

Articles you may be interested in

[Tunable phononic crystals based on piezoelectric composites with 1-3 connectivity](#)

J. Acoust. Soc. Am. **139**, 3296 (2016); 10.1121/1.4950725

[Guidance of surface waves in a micron-scale phononic crystal line-defect waveguide](#)

Appl. Phys. Lett. **106**, 081903 (2015); 10.1063/1.4913532

[Laminated piezoelectric phononic crystal with imperfect interfaces](#)

J. Appl. Phys. **111**, 013505 (2012); 10.1063/1.3672404

[On chip complex signal processing devices using coupled phononic crystal slab resonators and waveguides](#)

AIP Advances **1**, 041903 (2011); 10.1063/1.3676168

[Waveguiding in two-dimensional piezoelectric phononic crystal plates](#)

J. Appl. Phys. **101**, 114904 (2007); 10.1063/1.2740352

The advertisement features a blue background with a molecular structure graphic. On the left is a thumbnail of an 'Applied Physics Reviews' journal cover showing a 3D lattice structure. The main text reads 'NEW Special Topic Sections' in large white letters. Below this, it says 'NOW ONLINE' in yellow, followed by 'Lithium Niobate Properties and Applications: Reviews of Emerging Trends' in white. The AIP Applied Physics Reviews logo is in the bottom right corner.

NEW Special Topic Sections

NOW ONLINE
Lithium Niobate Properties and Applications:
Reviews of Emerging Trends

AIP Applied Physics
Reviews

Active wave-guiding of piezoelectric phononic crystals

Joo Hwan Oh, Il Kyu Lee, Pyung Sik Ma, and Yoon Young Kim^{a)}

WCU Multiscale Design Division, School of Mechanical and Aerospace Engineering, Seoul National University, 599 Gwanak-ro, Gwanak-gu, Seoul 151-744, Korea

(Received 20 June 2011; accepted 9 August 2011; published online 25 August 2011)

By numerical simulations, we show that active wave-guiding can be realized in a stop band frequency range of a phononic crystal (PC) if piezoelectric inclusions in the PC are electrically controlled. The advantages of the wave-guiding are that no permanent geometry or material change is needed and that somewhat arbitrarily shaped waveguides can be formed actively in PC structures. The analysis with supercells consisting of piezoelectrically coupled and decoupled inclusions shows that symmetric wave modes confined within the waveguide formed by decoupled inclusions are most responsible for wave transmission. © 2011 American Institute of Physics. [doi:10.1063/1.3630231]

Phononic crystals (PCs) exhibit interesting, useful phenomena such as band gap phenomena,¹ wave focusing,² and negative refraction.³ In particular, PC structures with crystal defects have recently received much attention because they allow the formation of propagating wave modes within a stop band frequency range of a PC structure and thereby the defected region can be used as a waveguide. Khelif *et al.*⁴ experimentally demonstrated the guiding of acoustic waves by removing rods from periodically arranged steel rods immersed in water. Pennec *et al.*⁵ analyzed the wave-guiding phenomena in a PC structure made up of cylinder dots on a thin plate having different geometries or materials. Oudich *et al.*⁶ studied guided modes in locally resonant phononic crystal waveguides having various widths. More results on phononic crystal waveguides may be found in Refs. 7–11.

If a PC waveguide is actively created, i.e., tunable, permanent installation of a defect can be avoided. In fact, PC-based tunable waveguides can be achieved if an active material is used as an inclusion material. Some attempts^{12–15} to control band gaps by piezoelectric and/or magnetostrictive materials were made earlier. However, no investigation has been reported to use active piezoelectric materials for active wave-guiding, i.e., for forming somewhat arbitrarily shaped waveguides within a finite PC structure. Here, we propose active wave-guiding by controlling piezoelectric coupling effects of some of the piezoelectric inclusions in a PC structure. The main advantage of using piezoelectric inclusions for active wave-guiding among various active materials is that the coupling effect of each piezoelectric inclusion can be controlled independently by connecting a separate circuit to each of the piezoelectric inclusions forming a waveguide. After showing the feasibility of the suggested active wave-guiding approach by numerical simulations, we will then investigate the physics explaining how the active wave-guiding is possible. For the investigation, an emphasis is put on the guided modes formed within an actively created waveguide.

The PC structure considered in this work has PZT (lead zirconate titanate)-5A rods embedded in a bulk silicon matrix:¹⁶ see Fig. 1(a). The constitutive equation of a piezoelectric material can be written as

$$\mathbf{T} = \mathbf{c}\mathbf{S} - \mathbf{e}^T\mathbf{E}, \mathbf{D} = \mathbf{e}\mathbf{S} + \boldsymbol{\epsilon}\mathbf{E}, \quad (1)$$

where \mathbf{T} , \mathbf{S} , \mathbf{E} , and \mathbf{D} represent stress, strain, electric field, and electric density, while the coefficients \mathbf{c} , \mathbf{e} , and $\boldsymbol{\epsilon}$ denote the elastic stiffness, piezoelectric coupling coefficient, and electric permittivity, respectively. Here, the coupling coefficient \mathbf{e} can be regarded to vanish, resulting in a decoupled state when the external electrical circuit connected to the piezoelectric rod is closed. Obviously, the dispersion relation of the PC will be different depending on the piezoelectric stiffening effect affected by the piezoelectric coupling state.^{12,13} Under the assumption of the piezoelectric polling in the z direction, one can mainly focus on out-of-plane displacement modes because in-plane modes are not affected by the piezoelectric coupling state.¹²

The dispersion curves of the PC with piezoelectrically coupled and decoupled inclusions (will be referred to as the coupled and decoupled PC) calculated by the finite element

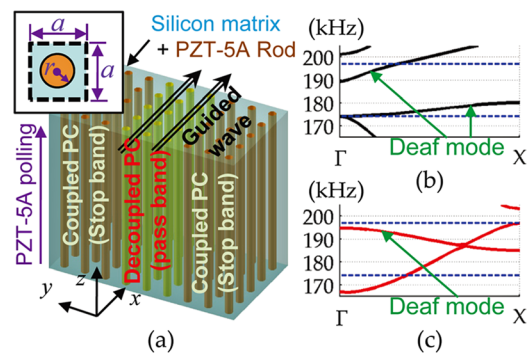


FIG. 1. (Color online) (a) Schematic illustration of a PC structure (a : 16 mm, r : 6 mm) having piezoelectric rod inclusions, forming a tunable straight waveguide. (b) The dispersion relations of the coupled PC and (c) those of the decoupled PC. (The non-zero values of the coupling coefficient of the used PZT-5A are $e_{31} = e_{32} = -5.3576$, $e_{33} = 15.7835$, and $e_{15} = e_{24} = 12.2947$ (unit: C/m²)).

^{a)}Author to whom correspondence should be addressed. Electronic mail: yykim@snu.ac.kr. Phone: +82-2-880-7154. Fax: +82-2-872-1513.

method¹⁷ are shown in Figs. 1(b) and 1(c). From the dispersion curves in the frequency range between 174 and 197 kHz (between the blue dotted lines in Figs. 1(b) and 1(c)), only deaf modes¹⁸ exist in the coupled PC while both deaf and propagating modes exist in the decoupled PC. Since such deaf modes cannot be excited by incident plane waves, no wave can actually propagate through the coupled PC while the decoupled PC allows an incident plane wave to pass through. To demonstrate how this finding can be used to form an active, somewhat arbitrarily shaped waveguide, numerical simulations were performed.

Fig. 2(a) shows the finite element modeling for a straight waveguide formed by three finite arrays of the decoupled PC surrounded by the coupled PC. The total number of PZT-5A rods embedded in a silicon matrix is 25×25 . To form a waveguide for a selected frequency of 185 kHz lying in the band gap of the coupled PC, a closed electric circuit is connected to each of all PZT-5A rods located along the desired wave path while the surrounding coupled PC provides a stop band due to the imposed open electric circuit condition. The upper left figure in Fig. 2(b) shows that the incident wave propagates mainly through the decoupled PC region colored

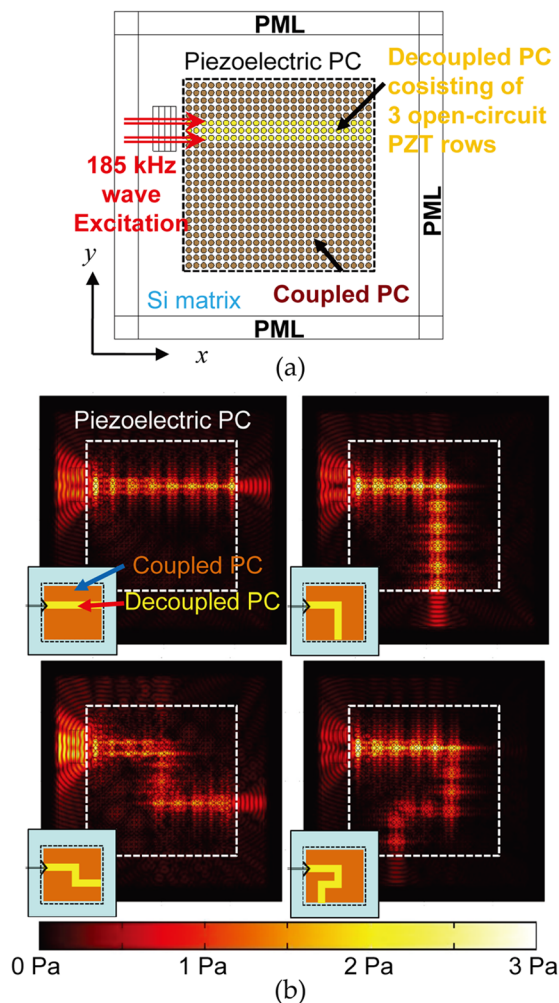


FIG. 2. (Color online) (a) Finite element model for simulating wave transmission in a tunable PC having unit cell shown in Fig. 1(a). Here, the case of a linearly formed waveguide is illustrated. (b) The von Mises stress distributions for four different waveguides that are actively created by controlling the electric circuit states for all piezoelectric rods.

yellow. This is mainly because the coupled PC surrounding the waveguide has a stop band, resulting in the confinement of the wave within the decoupled PC region. Also, the three remaining figures in Fig. 2(b) demonstrate that quite arbitrarily shaped decoupled PC waveguides can be indeed formed by controlling the piezoelectric coupling states of the corresponding piezoelectric rods. Although the results in Fig. 2(b) were based on PC having infinite thickness, the numerical simulations with PC plates having a finite thickness of 2 mm subject to an anti-symmetric flexural guided wave excitation also exhibited high tunability of the PC structure. Thus, the findings from this study can be also applied to thin plate PC structures.

To investigate how incident plane waves can propagate through the decoupled PC region, the characteristics of the guided modes are investigated by employing the supercell shown in Fig. 3(a), as done in Ref. 10. Figs. 3(c) and 3(d) show the dispersion curve of the guided modes for the frequency range corresponding to the stop band of the coupled PC while Fig. 3(b) shows the mode shapes of the modes. In Fig. 3(b), the symbols “ S_n ” and “ A_n ” denote the n th symmetric and anti-symmetric modes with respect to the

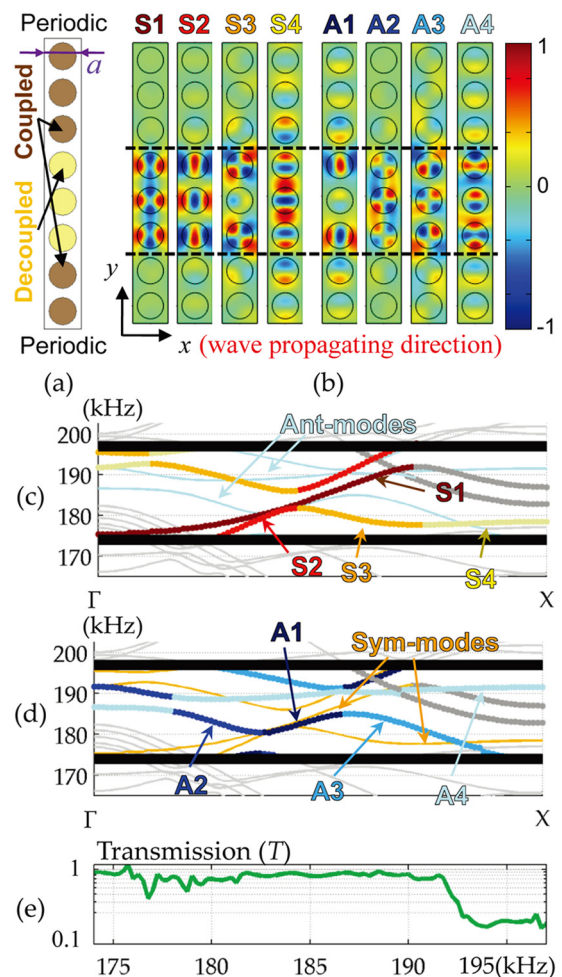


FIG. 3. (Color online) (a) A supercell consisting of the silicon matrix and 8 piezoelectric rods. Three central rods are in a piezoelectrically decoupled state while the others, in a coupled state. (b) Mode shapes of the supercell with dominant out-of-plane displacements within the actively created waveguide. (c) Dispersion curves of symmetric guided modes and (d) those of anti-symmetric guided modes. (e) Transmission of the PC structure having a straight waveguide.

horizontal axis passing through the center of the 3 decoupled PC region. The mode order number, n , is so arranged that modes with larger numbers have more sign changes in their out-of-plane displacement distributions. Note that since only the S1, A2, and A4 modes exist at the target frequency of 185 kHz, other mode shapes shown in Fig. 3(b) are plotted at different frequencies: S2, S3, and S4 at 178 kHz while A1 and A3 at 183 kHz. Nevertheless, within the frequency range, the patterns of the modes are almost the same.

To check the transmission through the actively created waveguide, a measure of transmission defined as $T = |\bar{U}_T|/|\bar{U}_I|$ (Ref. 19) is plotted in Fig. 3(e). Here, \bar{U}_T is the averaged out-of-plane displacement of the transmitted wave calculated at the output port of the active waveguide¹⁰ while \bar{U}_I , the counterpart at the input port. For the simulation of T , 15 layers of the supercell in Fig. 3(a) are placed along the x direction as in Ref. 10, and a plane wave having out-of-plane time-harmonic displacement motion is assumed to be incident on the left end of the actively created waveguide. To calculate \bar{U}_I , the two-point method²⁰ is employed, and it is remarked that although T may exceed unity, it describes the physics of wave transmission properly.¹⁹

By using the results obtained in Figs. 3(b)–3(e), the following findings regarding the wave transmission through the actively created waveguide are summarized:

1. Guided modes confined mainly in the waveguide are created upon switching on the electric circuit connected to piezoelectric rods lying in a selected waveguide.
2. Although all branches participate in carrying the plane wave, the S1 mode plays the dominant role because its out-of-plane displacement mode shape along the y direction resembles most the plane wave. However, other modes can significantly participate in wave transmission for an angled waveguide.
3. Lower modes have shorter wavelengths in the propagating x direction than higher modes. For instance, the wavelength of the S1 mode is approximately $2a/3$ while that of the S4 mode, $2a$. This indicates that the S1 mode belongs to a higher Brillouin zone while the S4 mode, to a lower Brillouin zone and also that the S1 branch starts from a lower cut-off frequency than the S4 branch.
4. The S1 mode has a zero group velocity around 192 kHz, from which a partial band gap is formed. This explains why the transmission shown in Fig. 3(e) drops rapidly around the frequency of 192 kHz.

A few more remarks on other branches that are not marked with S_n or A_n may be made. The branches expressed in thick gray lines in Figs. 3(c) and 3(d) result from the deaf modes of the coupled PC while other gray branches are due to the imposition of the periodic condition along the y axis. (Therefore, all of these branches do not participate in wave transmission along the waveguide.) Finally, the simulation with narrower waveguides, i.e., with the reduced number of the piezoelectric rods forming the waveguide from 3 to 1, shows that only the lowest few modes (S1, S2, and A1) remain to survive due to the increase of the cut-off frequencies. This result agrees with the previous study¹⁰ which

showed the disappearance of higher modes with a narrower PC waveguide. However, the transmission in narrower waveguides would be considerably reduced, especially in case of bent waveguides.

This study suggests that if piezoelectric inclusions are used to form a PC, one can form quite arbitrarily shaped waveguides actively. Because the coupled PC has a stop band only along the $\Gamma - X$ direction in the selected frequency range, a waveguide can be composed only of vertical and horizontal segments. Nevertheless, the use of piezoelectric materials allows relatively easy control of the piezoelectric coupling state independently for each piezoelectric rod, so fine wave-guiding can be possible. The proposed wave-guiding approach may be utilized to make elastic wave routers. The dispersion and wave mode analyses with a supercell explain how incident plane waves can propagate through the waveguide.

This work was supported by the National Research Foundation of Korea (NRF) grant (No: 2011-0017445) funded by the Korean Ministry of Education, Science and Technology (MEST) contracted through IAMD at Seoul National University and WCU program (No. R31-2010-000-10083-0) through NRF funded by MEST.

¹M. S. Kushwaha, P. Halevi, L. Dobrzynski, and B. Djafari-Rouhani, *Phys. Rev. Lett.* **71**, 2022 (1993); M. Sigalas and E. N. Economou, *Solid State Commun.* **86**, 141 (1993).

²C.-Y. Chiang and P.-G. Luan, *J. Phys.: Condens. Matter* **22**, 055405 (2010); E. A. Vinogradov, V. A. Babintsev, V. G. Veselago, and K. F. Shpilov, *Phys. Wave Phenom.* **15**, 126 (2007).

³M. K. Lee, P. S. Ma, I. K. Lee, H. W. Kim, and Y. Y. Kim, *Appl. Phys. Lett.* **98**, 011909 (2011); B. Morvan, A. Tinel, A.-C. Hladky-Hennion, J. Vasseur, and B. Dubus, *Appl. Phys. Lett.* **96**, 101905 (2010); J. Bucay, E. Roussel, J. Vasseur, P. Deymier, A. C. Hladky-Hennion, Y. Pennec, K. Muralidharan, B. Djafari-Rouhani, and B. Dubus, *Phys. Rev. B* **79**, 214305 (2009).

⁴A. Khelif, A. Choujaa, S. Benchabane, B. Djafari-Rouhani, and V. Laude, *Appl. Phys. Lett.* **84**, 4400 (2004).

⁵Y. Pennec, B. Djafari Rouhani, H. Larabi, A. Akjouj, J. Gillet, J. Vasseur, and G. Thabet, *Phys. Rev. B* **80**, 144302 (2009).

⁶M. Oudich, M. B. Assouar, and Z. Hou, *Appl. Phys. Lett.* **97**, 193503 (2010).

⁷H. Chandra, P. Deymier, and J. Vasseur, *Phys. Rev. B* **70**, 054302 (2004).

⁸X. Li and Z. Liu, *Phys. Lett. A* **338**, 413 (2005).

⁹J.-H. Sun and T.-T. Wu, *Phys. Rev. B* **71**, 174303 (2005).

¹⁰A. Khelif, B. Djafari-Rouhani, J. Vasseur, and P. Deymier, *Phys. Rev. B* **68**, 024302 (2003).

¹¹T.-C. Wu, T.-T. Wu, and J.-C. Hsu, *Phys. Rev. B* **79**, 104306 (2009).

¹²Z. Hou, F. Wu, and Y. Liu, *Solid State Commun.* **130**, 745 (2004).

¹³M. Wilm, A. Khelif, V. Laude, and S. Ballandras, *J. Acoust. Soc. Am.* **122**, 786 (2007).

¹⁴J. F. Robillard, O. B. Matar, J. O. Vasseur, P. A. Deymier, M. Stippinger, A. C. Hladky-Hennion, Y. Pennec, and B. Djafari-Rouhani, *Appl. Phys. Lett.* **95**, 124104 (2009).

¹⁵Y.-Z. Wang, F.-M. Li, W.-H. Huang, X. Jiang, Y.-S. Wang, and K. Kishimoto, *Int. J. Solids Struct.* **45**, 4203 (2008).

¹⁶Material properties for PZT-5A and silicon used in this work are from comsol Material Library.

¹⁷P. Langlet, A.-C. Hladky-Hennion, and J.-N. Decarpigny, *J. Acoust. Soc. Am.* **98**, 2792 (1995).

¹⁸F.-L. Hsiao, A. Khelif, H. Moubchir, A. Choujaa, C.-C. Chen, and V. Laude, *J. Appl. Phys.* **101**, 044903 (2007).

¹⁹P. Lambin, A. Khelif, J. Vasseur, L. Dobrzynski, and B. Djafari-Rouhani, *Phys. Rev. E* **63**, 066605 (2001).

²⁰B. Lundberg and A. Henchoz, *Exp. Mech.* **17**, 213 (1977).